*Anal. Bioanal. Electrochem.*, Vol. 5, No. 4, 2013, 506 - 516

**Analytical & Bioanalytical Electrochemistry**



*Full Paper*

# Effect of First-Stage Temperature on the Hydrothermal Synthesis of Flower-Like Lithium Iron Phosphate

**Mohadese Rastgoo-Deylami[1,2], Mehran Javanbakht[1,2,*], Mehdi Ghaemi[2,3], Hamid Omidvar[2,4] and Hossein Ghafarian[1,2]**

[1] *Department of Chemistry, Amirkabir University of Technology, Tehran, Iran*

[2] *Renewable Energy Research Center, Amirkabir University of Technology, Tehran, Iran*

[3] *Department of Chemistry, Science faculty, Golestan University, Gorgan, Iran*

[4] *Department of Mining and Metallurgical Engineering, Amirkabir University of Technology, Tehran, Iran*

*Corresponding Author, Tel:.+98-2164542764; Fax: +98-21 64542762
E-Mail: mehranjavanbakht@gmail.com

*Received: 8 July 2013 / Received in revised form: 28 July 2013 /Accepted: 5 August 2013 / Published online: 30 August 2013*

---

**Abstract**- A controllable synthesis of flower-like lithium iron phosphate $LiFePO_4$ (LFP) was obtained via a two-stage heating during hydrothermal process. In the first stage, the temperature was held at 105 °C (LFP1), 120 °C (LFP2), 150 °C (LFP3) and 190 °C (LFP4) for 5 h. In the final stage, the temperature was held constant at 400 °C under $H_2/N_2$ atmosphere for 4 h. To increase the electrochemical reversibility and electronic conductivity, LFP is treated with polyethylene glycol (PEG) as the templating agent and carbon sources for the as-prepared materials. This is to obtain a modified LFP cathode with optimum electrical contact between the electroactive materials and the carbon-filled electrode matrix which is found to be effective in terms of raising the electrochemical performance of the Li-ion batteries. Results show that as the first-stage temperature increased, the corresponding electrochemical performance of the resulting sample has been increased up to a temperature of 150 °C. Galvanostatic charge-discharge test indicates that flower-like $LiFePO_4$/C composite, LFP3, exhibits initial discharge capacity of 118 mAh $g^{-1}$ at 0.1C rates. The performance improvement was attributed to a reduction of the thickness and particle size of the flower-like $LiFePO_4$ particles. Results of X-ray diffraction (XRD) revealed that the structure of the latter represents phase of the ordered olivine structure without any impurities. Cyclic voltammetry indicates that the improvement in redox cycling could be attributed to an increase of the electrochemical active surface area (ECSA) and the related increase in micro-porosity as evidenced by SEM analysis.

**Keyword-** Lithium Iron Phosphate ($LiFePO_4$), Hydrothermal Synthesis, Polyethylene Glycol, Flower-Like Morphology

## 1. INTRODUCTION

In recent years, environmental issues and synthesis of materials with specific biological properties, morphologies and sizes have been attracting great interest because of their potential applications in advanced functional materials. Hence, the development of new strategies for controlling the morphologies could be of great importance to increase the performance of rechargeable Li-ion batteries. These batteries are power sources for use in electric vehicles (EVs) and hybrid electric vehicle (HEVs) applications [1-4]. High capacity lithium transition-metal oxides and their derivatives, such as layered $LiCoO_2$, $LiMnO_2$, and $LiNiO_2$, spinel $LiMn_2O_4$, lithium iron phosphate ($Li_{1-y}FePO_4$) and so on have been widely studied. Olivine structure of $LiFePO_4$ (LFP), which is regarded as cathode material for Li ion battery, can be considered as the hexagonal structural analogue of spinel [5-7]. The Fe atoms in $LiFePO_4$ occupy the zigzag chains of octahedral and the Li atoms occupy the linear chains of the alternate planes of octahedral sites. Removal of all the lithium atoms leaves the layered $FePO_4$-type structure, which has the same Pnma orthorhombic space group. The $LiFePO_4$ charge process can be broadly described as:

$$LiFePO_4 \rightarrow Li_{(1-X)}FePO_4 + xLi^+ + xe^-$$

Due to its attractive characteristics, such as good electrochemical property, high thermal stability and environmental benignity, LFP is being recognized as a new and suitable positive-electrode material. This is due to its high theoretical capacity of 170 m $Ah.g^{-1}$, good thermal stability, low starting material cost and nontoxicity. It represents a along flat potential at 3.4 V (*vs*. $Li/Li^+$) during charge and discharge, which makes it suitable for high-power and large scale battery applications [8,9]. However, $LiFePO_4$ shows also poor electronic conductivity (only $10^{-9}$-$10^{-10}$ S $cm^{-1}$) and slow diffusion of $Li^+$ ion into $LiFePO_4$ structure [10]. Compared to other materials, the electronic conductivity of LFP is being much lower than those of $LiCoO_2$ (~ $10^{-3}$ S $cm^{-1}$) and $LiMn_2O_4$ ($2\times10^{-5}$-$5\times10^{-5}$ S $cm^{-1}$) [11,12]. Hence, much effort has been made to evaluate electrochemical activity of this material. These are based on particle size reduction [13-15], electronic conductive carbon coating [16,17] and metal-ion doping ($Al^{3+}$,$Zr^{4+}$, $Nb^{5+}$, $Ni^{2+}$ ) [18-26]. Another solution to this problem could be the surface modifications with metal nanoparticle coatings such as silver and copper as well as dispersion and intimate contact with highly conductive carbon particles. These would clearly increase the electric contact between the LFP particles and increase the performance of the corresponding cathode composite [27-29].

Various synthetic methods such as carbothermal reduction method [30], sol-gel process [31], solid-state reaction [32], co-precipitation method [33,34] and hydrothermal reaction [35-37] have been used for the synthesis of $LiFePO_4$. Whittingham et al. [38] also demonstrated the hydrothermal synthesis of $LiFePO_4$ using $FeSO_4.7H_2O$, $H_3PO_4$ and LiOH as starting materials. Morphology control, homogeneous particle size distribution, low cost, high crystallization of product and simplicity are advantages of hydrothermal method. In this method, temperature can affect the crystal growth process and crystallinity significantly. Hence, we examined different first stage temperatures ranging from 105-190 $^oC$ for the synthesis of precursor materials. Results show the temperature of the first stage must be controlled in order to control of the $LiFePO_4$ growth kinetics. The preliminary results of this study led us to the conclusion that further optimizing of the preparation conditions may result in more precise control of the physicochemical properties of the obtained flower-like $LiFePO_4$.

## 2. EPERIMENTAL

### 2.1. Synthesis of flower-like $LiFePO_4$ samples

$LiFePO_4$ was prepared via a hydrothermal route from starting materials $FeSO_4.7H_2O$, $H_3PO_4$ and $LiOH.H_2O$ in a molar ratio of 1:1:3. First $FeSO_4.7H_2O$ aqueous solution was mixed with $H_3PO_4$ at vigorous agitation. The drop wise addition of $LiOH.H_2O$ resulted in the formation of a sticky mixture. Polyethylene glycol (PEG: mean molecular weight of 380-420 g $mol^{-1}$), 32 ml, was added as surfactant. The pH value of the solution, in the order of 7.14, was obtained by dropping NaOH to the starting materials. The resulting mixture was quickly transferred in to 100-ml-capacity stainless steel autoclave with Teflon lining. The autoclave was sealed and the dead volume was purged with nitrogen to overcome undesired oxidizing reactions. The temperature in the first stage was held at 105 ºC (LFP1), 120 ºC (LFP2), 150 ºC (LFP3) and 190 ºC (LFP4) for 5h. Subsequently, the autoclave was cooled down to room temperature. Precipitate was collected by suction filtration and was washed several times with deionized water, dried in oven at 100 ºC for 3 h. In the second stage, LFP samples were heated at 400 ºC for 4 h in $H_2/N_2$ atmosphere (5 vol. % $H_2$ and 95 vol. % $N_2$) in order to remove the adsorbed water.

### 2.2. Preparation of $LiFePO_4$ electrode

The electrochemical properties of the Lithium iron phosphate cathode was performed in a three electrode conventional cell, which was assembled in a glove box filled with an argon atmosphere. The electrode was comprised of the electroactive LFP sample, ultra-pure graphite powder (purity>99.99 wt.%, Aldrich) and polytetrafluoroethylene (PTFE) as a binder in a weight ratio of 7.5:2.0:0.5. This blend was then rolled and pressed onto an

aluminum current collector. Subsequently, after drying in oven at 110 $^{o}$C for 12 h, the electrodes were soaked in electrolyte for 24 h. Lithium plates, cut from lithium metal ingots, were used for both counter and reference electrodes. The same electrolyte was used in all electrochemical tests, which was composed of 1 M $LiClO_4$ in a 1:1 weight ratio mixture of ethylene carbonate (EC) and dimethyl carbonate (DMC).

### 2.3. Characterization techniques

XRD (Equinox 3000) and Cu $K_\alpha$ radiation ($\lambda$=0.15418 nm) were used to study the phase composition of the prepared samples. The sample was scanned from 15$^{o}$ to 65$^{o}$ (2$\Theta$) with a speed of 3$^{o}$ min$^{-1}$. All samples were characterized in terms of morphology and particle size by SEM (Philips XL 30). The CV, EIS measurements and electrochemical charge/discharge test have been carried out using Galvanostat/Potentiostat Autolab (PGSTAT 302N).

## 3. RESULTS AND DISCUSSION

Fig. 1 exhibits the SEM images of the LFP products showing a flower-like morphology with different particle- size and thicknesses. From the images, it is apparent that raising the first stage temperature up to 190 $^{o}$C encourages the formation of smaller grains. Fig. 1a shows the SEM micrograph of the LFP1 sample, which is prepared in the first stage at 105 $^{o}$C. This reveals that this sample consist of micron sized rods, which are self-assembled to form flower-like bundles. Generally, the hydrothermal process is controlled by the dissolution/recrystallization mechanism. If the probability of the crystal nucleation is higher than that of the crystal growth, the crystals will be small; otherwise they will be large. Obviously, the morphology and particle size of $LiFePO_4$ is also dependent on drying temperature, time and concentration of starting materials [38]. It could be assumed that the release of molecular water from the solid matrix play significant role in the growth kinetics. This indicates that different processes control the growth kinetics at different stages of the synthesis. SEM shows that the increase in temperature does not change the flower morphology of LFP1, LFP2 and LFP3; however, at higher first stage temperature of 190 ºC, flower-like structure is destroyed, as in the case of LFP4.

Fig. 2 shows the X-ray diffraction patterns of LFP3 sample prepared hydrothermaly by using polyethylene glycol as the template and carbon source. The diffraction patterns exhibits no impurities and all peaks are identified to be those from orthorhombic olivine-type structure with the space group of Pnma. The PEG adsorbed on the surface of LFP particles, could passivate them against oxidation to some extent, which might be another possible reason that no impurities like Fe oxides or hydroxide were formed in LFP3 samples.

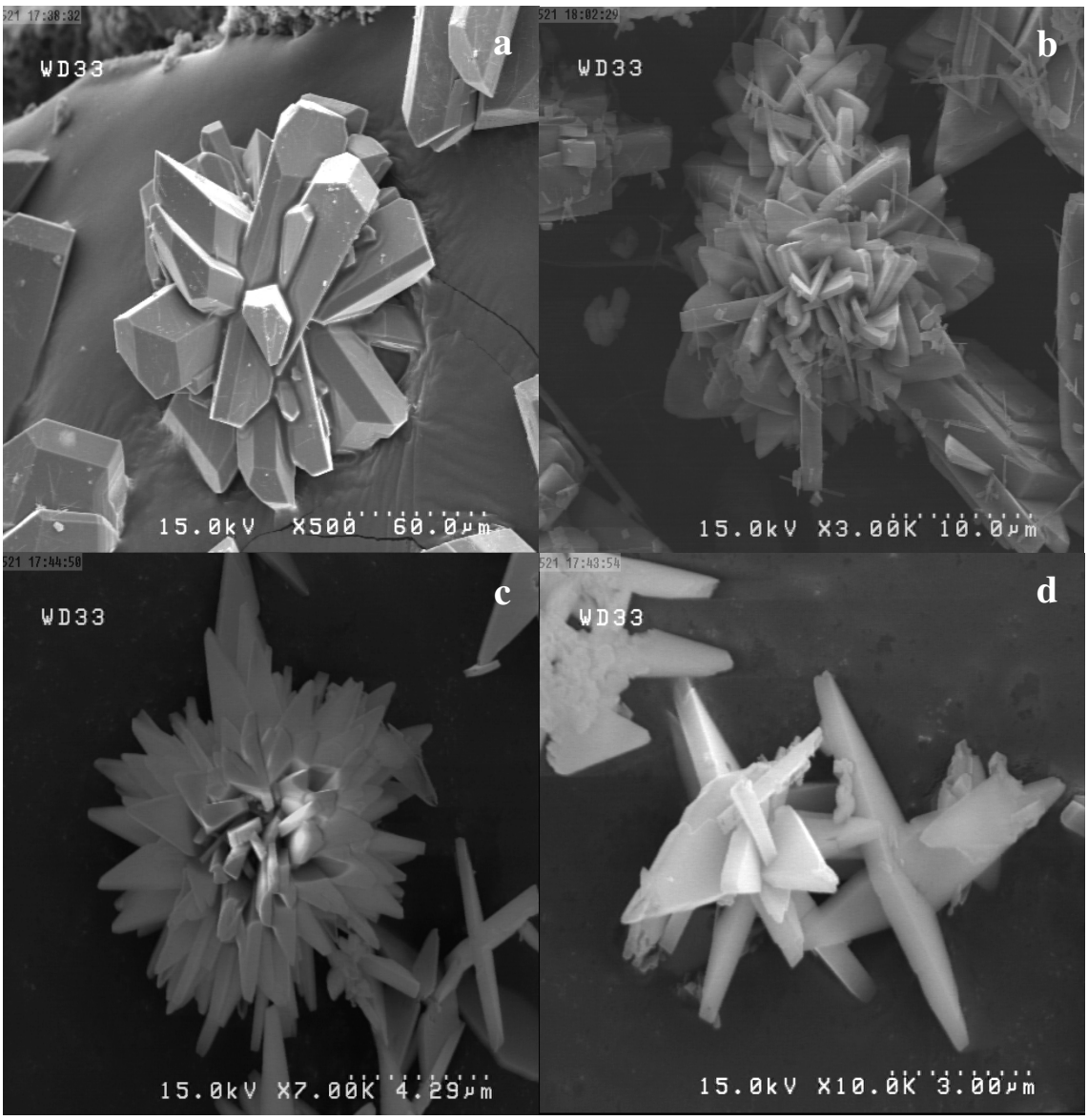


**Fig. 1.** SEM micrographs of a) LFP1, b) LFP2 , c) LFP3 and d)LFP4 samples, prepared by hydrothermal method followed by heating in $H_2/N_2$ atmosphere (5 vol. % $H_2$ and 95 vol. % $N_2$) at 400°C for 4 h

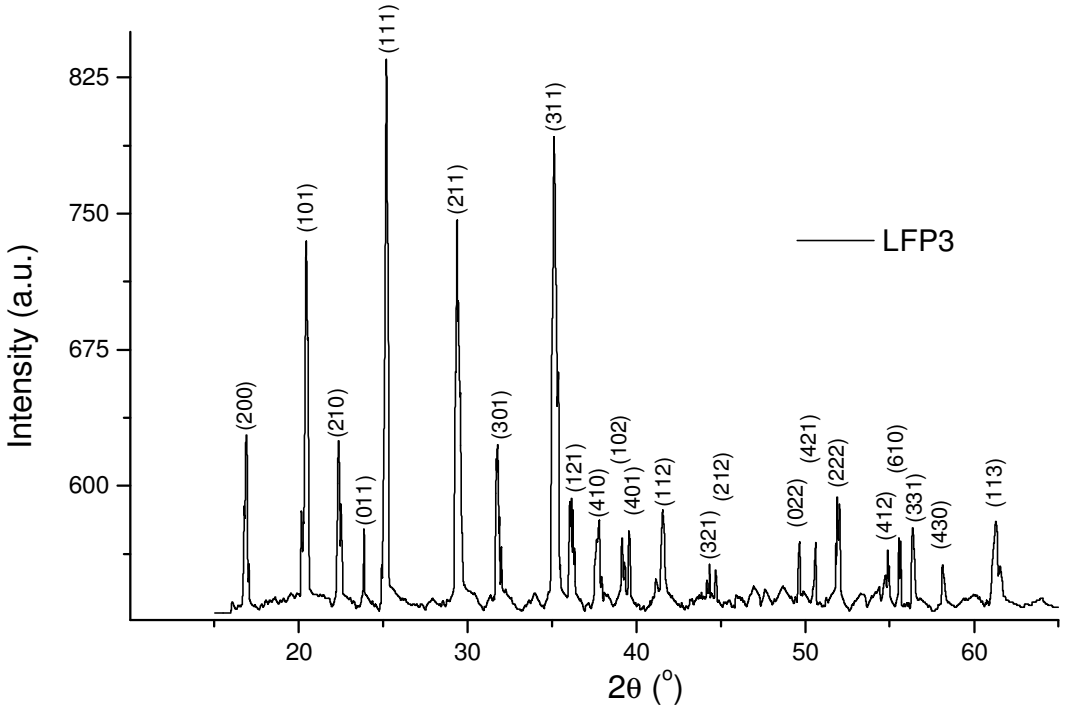


**Fig. 2.** X-ray powder diffraction patterns of the LFP3 samples

Cyclic voltammetry is a useful technique to evaluate the polarization and electrochemical reaction reversibility by measuring the magnitude of peak separation between anodic ($E_{pa}$) and cathodic ($Ep_c$) peak potentials [39]. CV measurements were performed in a potential range of 2.5-4.5 V at scanning rate of 0.1 mV $s^{-1}$. (Fig. 3). Anodic and cathodic peaks are corresponding to the two-phase charge/discharge reaction of $Fe^{2+}/Fe^{3+}$ redox couple. The LFP3 sample (Fig. 3), exhibits well-defined and symmetrical anodic peak potentials of 3.75 V and a corresponding cathodic response at 3.22 V *vs.* the $Li/Li^+$ reference electrode, respectively. The latter exhibits the highest peak current densities among other samples (not shown here), which could be partly attributed to a decrease in the thickness and the size of the obtained flower-like microcrystals. The potential separation between the two peaks is 0.53 V, which is representative of its good kinetics and electrochemical reaction reversibility. Anodic and cathodic peak currents are $3.21\times10^{-4}$ and $2.53\times10^{-4}$ A, respectively. The enhanced intercalation/de-intercalation kinetics of the sample could also be due to increased micro-porosity as evidenced by SEM.

A decrease in particle size leads to an increase in peak current ($i_p$) and decrease in peak separation. From cyclic voltammetry studies, it could be estimated that the LFP3 has higher electrochemical active surface area than other samples. Obviously, this area decrease at higher first stage temperature of 190 °C, as in the case of LFP4.

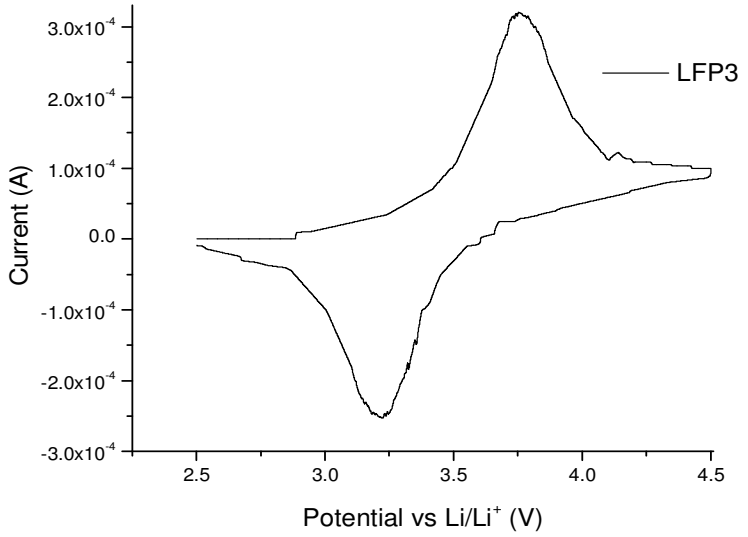


**Fig. 3.** Cyclic voltammograms of LFP3 sample in the first cycle at a scan rate of 0.1 mV $s^{-1}$ between the potential limit of 2.5 and 4.5 V (*vs.* $Li^+$/Li)

Nyquist plot (Fig. 4) are composed of a semicircle in the high frequency related to the charge-transfer resistance $R_{ct}$ of the $Li^+$ ions at the $LiFePO_4$/electrolyte interface. This is followed by an inclined warburg line in the low-frequency region, which is related to porous nature of cathode and diffusion of lithium ions within interior of the solid structure. The high-frequency intercept of the semi-circle on the real axis represents the ohmic resistance ($R_{sol}$). The lowest value of charge transfer resistance ($R_{ct}$), estimated from diameters of semicircles on Nyquist plots was measured for LFP3 in the order of 534.45 Ω.

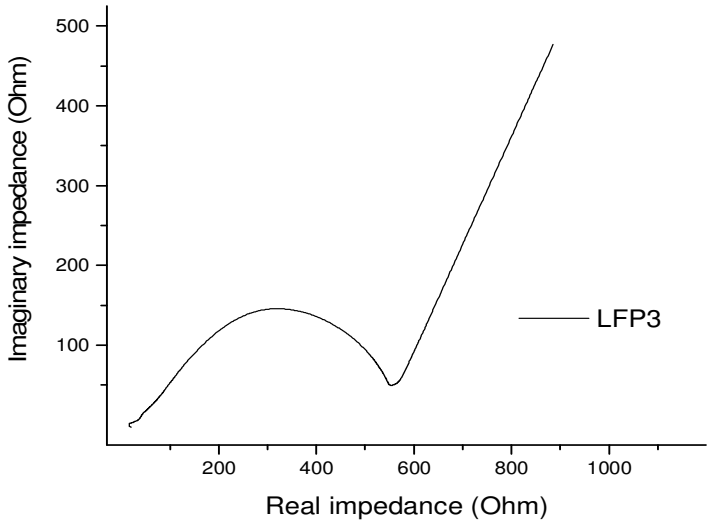


**Fig. 4.** Electrochemical impedance spectroscopy (EIS) results of LFP samples in the frequency range between 1 MHz and 10 mHz

Electrochemical performance of the $LiFePO_4$ sample was examined by galvanostatic charge–discharge tests under a current rate of 0.1 C. Fig. 5 displays the initial charge/discharge curve of the LFP3 sample in the potential range between 2.5 to 4.5 V. LFP3 showed a good flat discharge voltage at approximately 3.5 V, which represent the typical intercalation/deintercalation of $Li^+$ into the cathode craystal lattice. The small voltage difference between the charge and discharge plateaus is representative of its good kinetics. It is generally considered that smaller particles of $LiFePO_4$ are beneficial for the accessibility of $Li^+$ ions and result in lower total polarization. The latter sample gives the highest initial discharge capacity of 118 m Ah $g^{-1}$, which corresponds to over 70% of the theoretical capacity of olivine $LiFePO_4$. Other important factors affecting discharge capacities could be ascribed to the degree of crystallization, purity, porosity and the related electrolyte penetration [40].

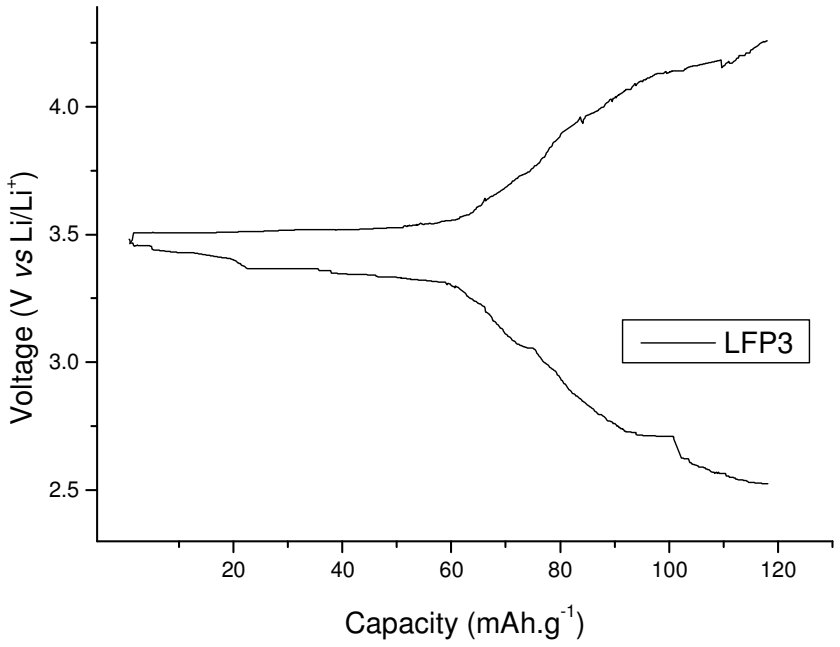


**Fig. 5.** Initial charge and discharge curves of LFP3 sample measured at the current density of 0.1 C in the potential range from 2.5 to 4.5 V

## 4. CONCLUSION

Flower-like $LiFePO_4$ microcrystals have been successfully obtained by a simple hydrothermal synthesis route. Synthesis was carried out in the presence of poly ethylene glycol, which acts as a carbon source, structure orienting agent and surface-modifying reagent. Results of this work showed that the first stage heat treatment of the precursor

material plays an important role in growth kinetics and electrochemical behavior of LFP cathode. The thickness and size of the growing crystallites could be easily controlled by varying the first stage temperature during hydrothermal synthesis. It provides a facile method for the preparation of $LiFePO_4$ cathode materials with well-developed flower-like morphology.

Performance improvement of the optimizes LFP3 could be related to a facilitated diffusivity of electroactive ions and reduced diffusion path length of $Li^+$ ions due to a more uniform and smaller crystal size of the flower-like microcrystals. This may support the penetration of electrolyte into micropores and ultimately increase lithium ion mobility within the oxide lattice.

**Acknowledgments**

The financial support of Amirkabir University of Technology and Iranian National Science Foundation (INSF) is greatly acknowledged.

**REFERENCES**

[1] P. Gibot, M. Casas-Cabanas, L. Laffont, S. Levasseur, P. Carlach, S. Hamelet, J. M. Tarascon, and C. Masquelier, Nat. Mater. 7 (2008) 741.
[2] M. Armand, J. M. Tarascon, Nature 451 (2008) 652.
[3] B. Kang, G. Ceder, Nature 458 (2009) 190.
[4] P. G. Bruce, B. Scrosati, and J. M. Tarascon, Angew. Chem. Int. Ed. 47 (2008) 2930.
[5] A. K. Padhi, K. S. Nunjundaswamy, and J. B. Goodenoygh, J. Electrochem. Soc. 144 (1997) 1188.
[6] A. S. Andersson, J. O. Thomas, B. Kalska, and L. Haggstorm, Electrochem. Solid State lett. 123 (2001) 563.
[7] S. T. Myung, S. Komaba, N. Hirosaki, H. Yashiro, and N. Kumagai, J. Electrochim Acta 9 (2004) 4213.
[8] M. S. whittingham, Chem. Rev. 104 (2004) 4271.
[9] S. Y Chung, J. T. Bloking, and Y. M. Chiang, Nat. Mater. 1 (2002) 123.
[10] Y. D. Cho, G. T. Fey, and H. M. Kao, J. Solid State Elecrochem. 12 (2008) 815.
[11] J. Molenda, A. Stoklosa, and T. Bak, Solid State Ionics 36 (1989) 53.
[12] Y. shimakawas, T. Numata, and J. Tabuchi, Solid State Chem. 131 (1997) 138.
[13] Y. G. Xia, M. Yoshio, and H. Noguchi, J. Electrochim. Acta 52 (2006) 240.
[14] K. Zaghib, P. Charest, M. Dontigny, A. Guerfi, and M. Lagace, J. Power Sources 195 (2010) 8280.

[15] E. M. Bauer, C. Bellitto, G. Righini, M. Pasquali, and A. Dell'Era, J. Power Sources 146 (2005) 544.
[16] S. W. Oh, S. T. Myung, S. M. Oh, K. H. Oh, K. Amine, B. Scrosati, and Y. K. Sun, Adv. Mater. 22 (2010) 4842.
[17] Y. H. Huang, and J. B. Goodenough, J. Chem. Mater. 20 (2008) 7237.
[18] M. Wagemaker, B. L. Ellis, D. Luetzenkirchen-Hecht, F. M. Mulder, and L. F. Nazar, J. Chem. Mater. 20 (2008) 6313.
[19] Z. J. Wu, H. F. Yue, L. S. Li, B. F. Jiang, X. R. Wu, and P. Wang, J. Power Sources 195 (2010) 2888.
[20] H. Liu, Q. Cao, L. J. Fu, C. Li, Y. P. Wu, and H. Q. Wu, J. Electrochem. Commun. 8 (2006) 1553.
[21] X. Q. Ou, G. C. Liang, L. Wang, S. Z. Xu, and X. Zhao, J. Power Sources 184 (2008) 543.
[22] S. Shi, L. Liu, C. Ouyang, D. S. Wang, Z. Wang, and L. Chen, Phys. Rev. 68 (2003) 195.
[23] D. Wang, H. Li, S. Shi, X. Huang, and L chen, Electrochem. Acta 50 (2005) 2955.
[24] G. X. Wang, S. L. Bewlay, K. Konstantinov, H. K. Liu, S. X. Dou, and J. H. Ahn, J. Electrochim. Acta 50 (2004) 443.
[25] M. R. Yang, W. H. Ke, and S. H. Wu, J. Power Sources 165 (2007) 646.
[26] S. Franger, C. Benoit, C. Bourbon, and F. L. Cras, J. Phys. Chem Solids 67 (2006) 1338.
[27] C. H. Mi, Y. X. Cao, X. G. Zhang, X. B. Zhao, and H. L. Li, Powder Technol. 181 (2008) 301.
[28] F. Croce, A. D. Epifanio, J. Hassoun, A. Deptula, T. Olczac, and B. Scrosati, Electrochem. Solid State Lett. 5 (2002) 47.
[29] K. S. Park, J. T. Son, H. T. Chung, S. J. Kim, and C. H. Lee, Solid State Commun. 129 (2004) 311.
[30] H. P. Liu, Z. X. Wang, X. H. Li, and H. J. Guo, J. Power Sources 184 (2008) 469.
[31] F. Yu, J. J. Zhang, Y. F. Yang, and G. Z. Song, J. Mater. Chem. 19 (2009) 9121.
[32] Y. H. Huang, J. B. Goodenough, J. Chem. Mater. 20 (2008) 7237.
[33] G. Arnold, J. Garche, R. Hemmer, and S. Strobele, J. Power Sources 119 (2003) 247.
[34] S. Franger, F. Le Cras, and H. Rouault, J. Power Sources 119 (2003) 252.
[35] W. Q. Huang, C. Qing, and X. Qin, J. Electrochem. 46 (2010) 16806.
[36] J. Chen, S. Wang, and M. S. Whittingham, J. Power Sources 174 (2007) 442.
[37] J. Chen, and M. S. Whittingham, J. Power Surces 8 (2006) 855.
[38] N. Recham, L. Dupont, M. Courty, K. Djellab, D. Larcher, and J. M Armand, Chem. Mater. 21 (2009) 1096.

[39] J. K. Kim, G. Cheruvally, J. H. Ahn, and H. J. Ahn, J. Electrochim. Acta 53 (2008) 8258.

[40] Y. Xia, W. Zhang, H. Huang, and Y. Gan, J. Power Sources 196 (2011) 5651.